Volume 17, Issue 3, 172521 (1-9)

Iranian Journal of Earth Science (IJES)

https://doi.org/10.57647/j.ijes.2025.16799

Application of stepwise fractal modeling for interpretation of remote sensing data, NE Iran

Hassan Saadati[1], Peyman Afzal[2,*], Habibollah Torshizian[3], Ali Solgi[1]

[1]*Department of Geosciences, SR.C., Islamic Azad University, Tehran, Iran.*
[2]*Department of Petroleum and Mining Engineering, ST.C., Islamic Azad University, Tehran, Iran.*
[3]*Department of Geology, Ma.C., Islamic Azad University, Mashhad, Iran.*

[*]**Corresponding author:** peymanafzal@gmail.com

Original Research

Received:
23 February 2024
Revised:
15 April 2024
Accepted:
22 June 2025
Published online:
10 July 2025

Abstract:

Remote sensing data is one of the common tools for recognition and separation index minerals of alteration zones especially clay minerals. In this study, an important clay mineral as named hectorite was detected by Spectral Angle Mapper (SAM) method based on ASTER data in a large region of NE Iran for reconnaissance of lithium ores. For this purpose, a proposed stepwise fractal modeling was used for determination and separation of the pixels with high intensity which can be shown the hectorite's zones. This process is used in three steps for reduction of zone's areas and extracted main hectorite zones. Based on results obtained by the stepwise fractal modeling in this region, the main anomalous zones for hectorite are located in the southern and SE parts of this region. Finally, the results derived via the stepwise fractal modeling were correlated with XRD data and field observations of the related clay minerals.

Keywords: Stepwise fractal modeling; Hectorite; Lithium; Remote sensing

1. Introduction

One of strategic metal of the world is lithium (Li) which is considered to be a green metal required for main technologies at 21th century. Sources of lithium included pegmatites, continental brines and hydrothermally altered clays (Munk et al., 2016). Due to increasing demand for lithium, regional exploration of this element is carried out in many countries (Kesler et al., 2012). Iran contains many granitic and pegmatite units and also there are many clay minerals and brines. Based on this potential, lithium resources can be explored and extracted economically in Iran (Saadati et al., 2020; Fyzollahhi et al., 2018). Lithium is associated with Be, Cs, Rb, Sc, W, Sn, Rare Earth Elements (REEs) and radioactive elements in granitic pegmatite rocks (London, 2008; Kesler et al., 2012).

Remote Sensing as a supplement to field lithological and structural mapping, has played an important role in the study of mineralized areas, since aerial photography became available in early 1950's (Sabins, 1999; Babaei and Sadeghi, 2010; Sadeghi et al., 2012). Satellite imagery can be successfully used for mineral reconnaissance. Satellite imagery have proved valuable for mineral exploration in three ways:

1. Mapping of regional and local fracture systems that controlled ore deposits.
2. Detection of surface alteration effects associated with ore deposits.
3. Providing basic data for geological mapping (Sadeghi et al., 2012).

The ASTER satellite image could be improved medium to high-spatial resolution and measured visible reflected radiation in three spectral bands between 0.52 and 0.86 μm in visible near infrared (VINIR) region (with 15-m spatial resolution), infrared reflected radiation in six spectral bands between 1.6 and 2.43 μm in shortwave infrared (SWIR) region (with 30-m spatial resolution) and thermal infrared

radiation in five spectral bands between 8.12 and 11.65 μm in thermal infrared (TIR) region (with 90-m spatial resolution). The ASTER data have been used to map silicate and carbonate rocks, as well as for volcanic studies, urban studies, lithological mapping, and monitoring of coastal environments (Rowan and Mars, 2003; Rahimzadegan et al., 2015). Researches proved the capability of the ASTER sensor in discriminating rock types and it is significantly used in identification of above mineral resources (**Amer et al.2010?**; Behbahani et al., 2023; Saed et al., 2022). These applications are under consideration of mining companies, exploration geologists, and mine owners for cost-benefit exploration and characterization of such economic important minerals, ore deposits, and rock types (Yazdi et al., 2018). The fractal methodology has been used to interpret each Classifiable data; such as geochemical, geophysical and remote sensing data. This approach is utilized simultaneously to separate anomalous zones determined by their concentrations or their intensity and occupied spaces (Afzal et al., 2017; Aliyari et al., 2020; Koohzadi et al., 2021; Heidari et al., 2024; Pourgholam et al., 2021; Sadeghi, 2021; Bazargani Golshan et al., 2025). As a well-known fractal approach, the concentration-area (C-A) fractal model, was proposed by Cheng et al. (1994) for anomalous area detection. Many researchers have been used and developed this method, e.g., (Khalajmasoumi et al., 2015; Khalajmasoumi et al., 2017; Afzal et al., 2022; Afzal et al., 2023).
In this article, hectorite's zones were detected via Spectral Angle Mapper (SAM) method and these zones were divided form the other geological units. Finally, obtained results were classified with the stepwise fractal modeling, and the high intensities for hectorites were selected. The stepwise fractal modeling is proposed in this study as an improved fractal model.

2. Geology

The Khorasan Razavi province is situated in the NE Iran which hosts many mineralization and several metallogenic belts (Fig. 1). The study region is bounded by a 600 km $\times$ 150 km Late Cretaceous to early Miocene Island arc set-

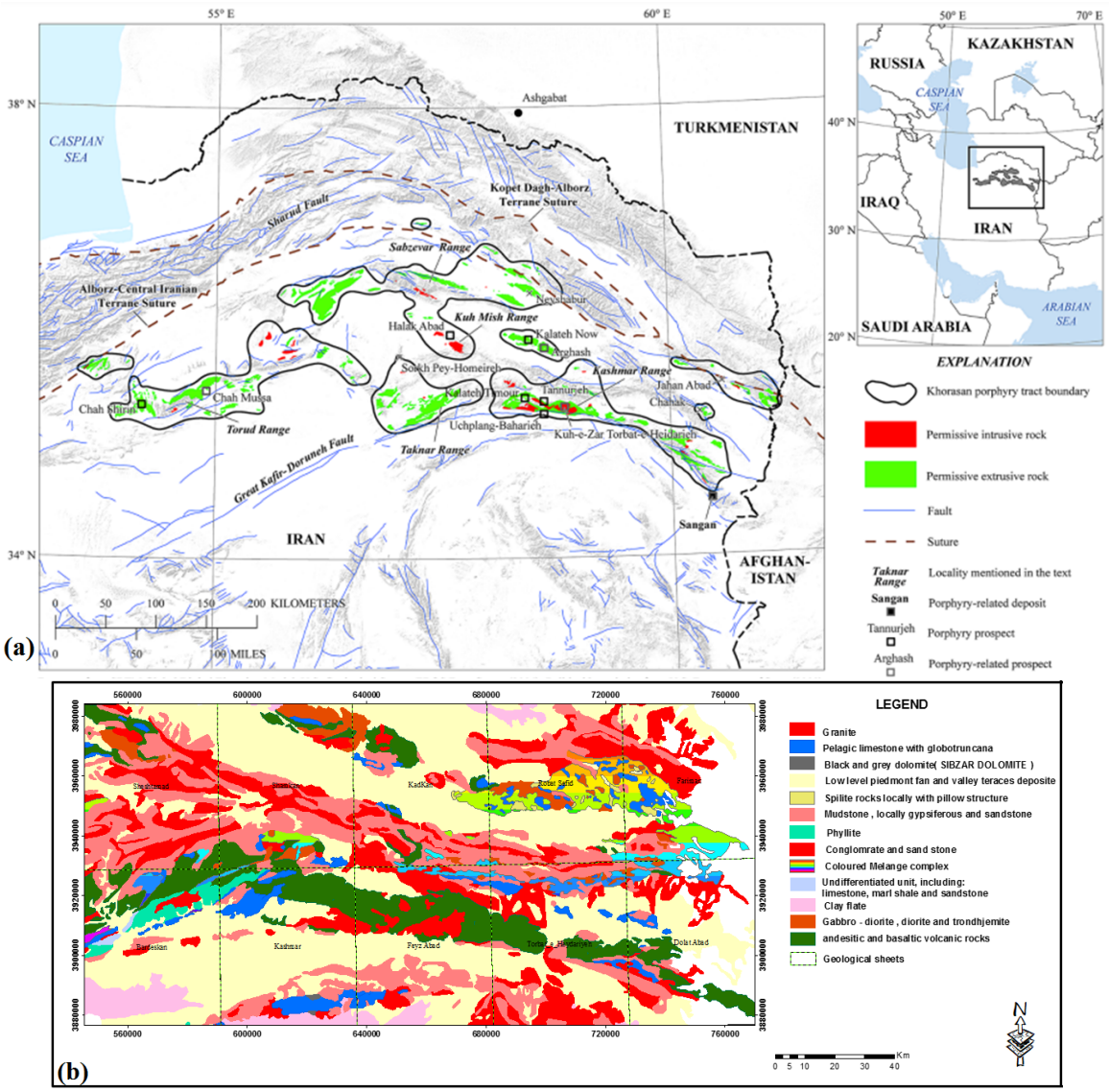

Figure 1. (a) The permissive intrusive and volcanic rocks with faults (A.A. et al., 2019); (b) Simplified geological map of the studied area (Modified based on A.A. et al. (2019))

ting. It overlies the NE extension of the Central Iranian terrane that divides the East Central Iranian Terrane, including Lut, Tabas, Kashmar-Kerman and Yazd terranes, along the left-lateral Great Kavir-Doruneh fault to the south (Arjmandzadeh et al., 2011; A.A. et al., 2019). Intrusive and volcano-plutonic rocks especially granitic units are extended in this region, as depicted in Fig. 2. Studied region contain ten 1:100000 sheets which are Sheshtamad, Shamkan, Kadkan, Robat Sefid, Fariman, Bardeskan, Kashmar, Feyz Abad, Torbat-e-Heydaryeh and Dolat Abad. There are Eocene and younger intrusives with granitic, pegmatitic, gabbro-dioritic, granodioritic, quartz-dioritic and monzodioritic compositions (A.A. et al., 2019). Furthermore, Late Cretaceous andesitic rocks and Early Eocene volcanosedimentary units extend in this region, as depicted in Fig. 2 (Miri Beydokhti et al., 2015; A.A. et al., 2019). In the northern and southern marginal parts of the studied district, Neogene clay minerals occurred and also, mudstones as absorbed minerals exist in many sectors of the studied region (Fig. 2). There are smectite, hectorite, illite and kaolinite with marls and mudstones which are similar to Hector mine in Nevada, USA (Kesler et al., 2012). There is porphyry, epithermal and other hydrothermal related deposits/occurrences (Malekzadeh Shafaroudi et al., 2013; A.A. et al., 2019). Mineralization in this region consists of porphyry ores, Late Cretaceous Cr-Mn ophiolite-related, Late Cretaceous-Eocene Volcanogenic Massive Sulfides (VMS) copper, Eocene red-bed copper, Eocene and Oligocene-Miocene precious metal epithermal deposits/mineralization (Karimpour et al., 2011). Azmi (2011) studied on the magmatic and sedimentary units for reconnaissance of Li resources in this region (Fig. 1). Saadati et al. (2020) carried out a geochemical exploration for Li using the geochemical mapping prospectivity index, staged factor analysis and fractal modeling. Based on Azmi (2011) and Saadati et al. (2020) studies, there are Li potentials in pegmatites, continental brines and altered clay minerals.

3. Materials and methods

3.1 Spectral Angle Mapper (SAM) method

Spectral angle mapping (SAM) method approach uses the angle of *n*-Dimensional vectors to compute the spectral similarities between the reference spectrums with the pixel spectrum (Kruse et al., 1993) the measures the spectral similarity by calculating the angle between two spectra (Rowan and Mars, 2003). A small angle between two spectra indicates high similarity and a large angle indicates low similarity and the amount of this measured angle is between zero and one. This method is not affected by the sun's radians factors, because the calculated angle between two vectors does not depend on the length of the two vectors. The *n* factor represents the available number of bands. SAM algorithm works quite well with the homogeneous pixels. Variations in the topographic illumination can be normalized effectively by using the SAM, but the ability to discriminate the rocks with the help of contrasting albedo is going to decreases and spectra is relatively flat (Cheng and Li, 2002; Jain and Sharma, 2019).

3.2 Concentration Area (C-A) fractal modeling

Cheng et al. (1994) proposed a C-A fractal model to delineate geochemical anomalies from the background. This method describes a reverse relationships between the elemental concentrations and the geological data, based on the amount of area that each specific concentration occupies in a study area; keeping in mind that by an increase in elemental concentration, the occupied area decreases. The C-A log-log plot use for this aim and different zones are separated based on exchange of straight lines' slopes (Cheng et al., 1994; Saed et al., 2022; Khalajmasoumi et al., 2015; Farhadi et al., 2022). This model has the general form of

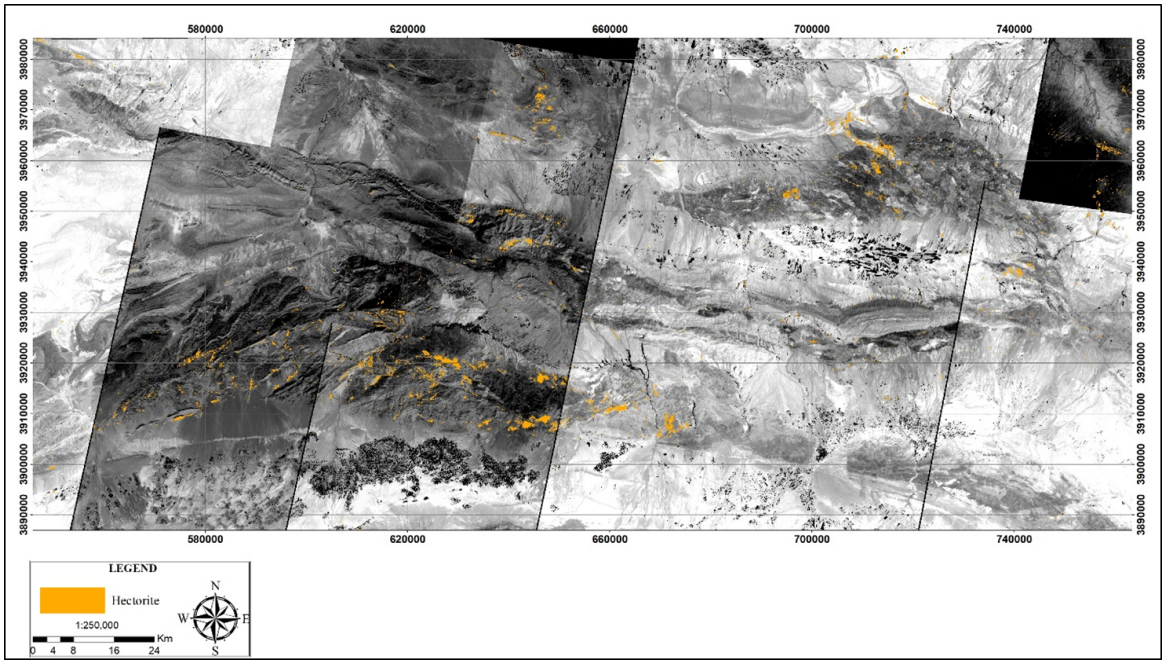

Figure 2. Hectorite dispersion in the exploration area revealed by the SAM method.

relation one as shown below (Cheng et al., 1994):

$$A(\rho \leq v) \infty \rho_1^{-\alpha};\ A(\rho \geq v) \infty \rho_2^{-\alpha} \quad (1)$$

Based on this equation, there is a reverse relationship between the attribute (pixel value in this study) and occupied areas. Many geological interpretations have been used by this method such as remote sensing data (Sadeghi et al., 2012; Behbahani et al., 2023).

3.3 Stepwise fractal modeling

The stepwise fractal modeling (SFM) is a method derived from the stepwise factor analysis which is a technique for extraction of significant multi-element anomalous signatures (Yousefi et al., 2019; Koohzadi et al., 2021). In this approach, to recognize the true high intensity of hectorite associations in a Li, non-indicator (noisy) pixels are progressively recognized and removed. Then, high intense pixels are detected and extracted in fractal modeling process. These pixels are main hectoritic units in area that could be contain Li ions in themselves. On the other hand, the main parts of the index mineral (hectorite in this scenario) were separated from other parts because fractal modeling is used in several stages and noisy pixels were removed in this progress. The stepwise fractal modeling, which is a method derived from the step-by-step factorial analysis of high intensity of pixel values.

The SFM can be included in exploration information system (EIS) to make its performance improved. The EIS provides spatial data analysis's tools and methods for mineral exploration (Yousefi et al., 2019; Yousefi and Hronsky, 2023). The SFM is an appropriate method for better interpretation of remote sensing data for alteration zones' detection.

4. Results

4.1 Application of Stepwise fractal modeling

In this research, ASTER satellite data were processed using SAM method with the aim of highlighting hectorite clays (Fig. 2). First, ASTER data were preprocessed based on radiometric, 2D/3D and vegetation mask. Vegetation indices are ratios calculated from reflectance measures in visible and near-infrared channels, which are used to estimate vegetation abundance in dark pixel corrected remote sensing images by the NDVI (Yazdi et al., 2018). Based on SAM method and spectral library, association of kaolinite, illite, montmorillonite, chlorite and hectorite were separated in spectral angle near to 0, e.g., 0.02 radian for chlorite. As a result of these processes, hectorite outcrops were seen mostly in the north and northeast as well as south and southwest parts of the exploration area. In the following, hectorite zones were classified and also checking the intensity of hectorite formation in hectorite zones. Then, the C-A fractal modeling was used investigate as well as possible and to identify the areas with the highest intensity of hectorite. The fractal modeling was used, and as a result of the three stages of fractal modeling, the areas with the highest intensity of hectorite in the range were determined. According to this model, the first statistical community includes pixels with a pixel value between 1 and 19, which are prominent in the southern parts of the target range. The second statistical community includes pixels with a pixel value between 19 and 50, which is located in the south and southeast parts of this community. The third statistical community includes pixels with a pixel value between 50 and 67, which is exposed in the south and southeast parts. The fourth statistical community includes pixels with a pixel value between 67 and 190. The pixels of this community are located in the southern parts of the region. The last statistical community of this region, which has the largest area in the range, has pixel values between 190 and 255, which are broken in the central, south, and southeast parts of the studied region (Fig. 3).

The second stage of modeling is applied to the pixels with high intensity so that among these pixels, more real intensity can be recognized. Based on this model, the first statistical population community includes pixels with a pixel value between 1 and 10, which are prominent in the southeast part of the target range. The second statistical community includes pixels with a pixel value between 10 and 32, which is located in the south and southeast parts of this community. The third statistical community includes pixels with a pixel value between 32 and 76, which is exposed in the south and southeast parts. The fourth statistical community includes pixels with a pixel value between 76 and 123 these pixels are scattered in the center, south, east, southeast and west parts of the research area. The fifth statistical community, includes pixels with a pixel value between 123 and 208 which are spatially identical to the pixels of the previous community. The last statistical community of this step, which has the largest area in the range, has pixel values between 208 and 255, which are mostly enhanced in the central, south, and southeast parts of the exploration area (Fig. 4).

The Final stage of modeling is applied to the pixels with high intensity so that among these pixels, more real intensity can be recognized. Based on this model, the first statistical population community includes pixels with a pixel value between 1 and 19, which are prominent in the South, North and NE part of the target region. The second statistical community includes pixels with a pixel value between 19 and 50, which are weakly exposed in the southeastern part of the study area. The third statistical community includes pixels with a pixel value between 50 and 67, which is exposed weakly in the south and north parts. The fourth statistical community includes pixels with a pixel value between 67 and 190 these pixels are scattered in the north, south, southeast and west parts of the research area. The last statistical community, which is the main area in the range, has pixel values between 190 and 255, which are mostly enhanced in the south, and southeast parts of the exploration area (Fig. 5).

5. Discussions

5.1 Correlation of remote sensing data with field and XRD analysis

In order to verify the data obtained from remote sensing studies, 27 samples were taken for XRD studies from the southern parts with the highest degree of hectorite intensity

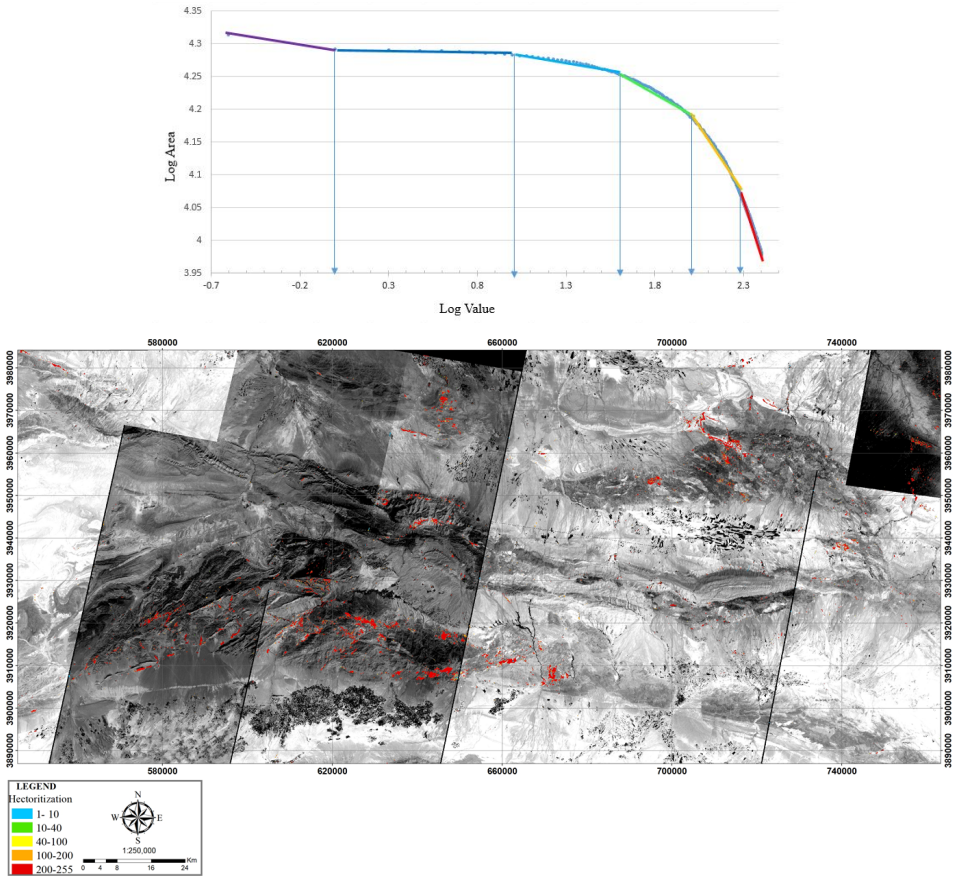

Figure 3. The Log-Log C-A fractal diagram and first stage of hectorite model based on SAM method.

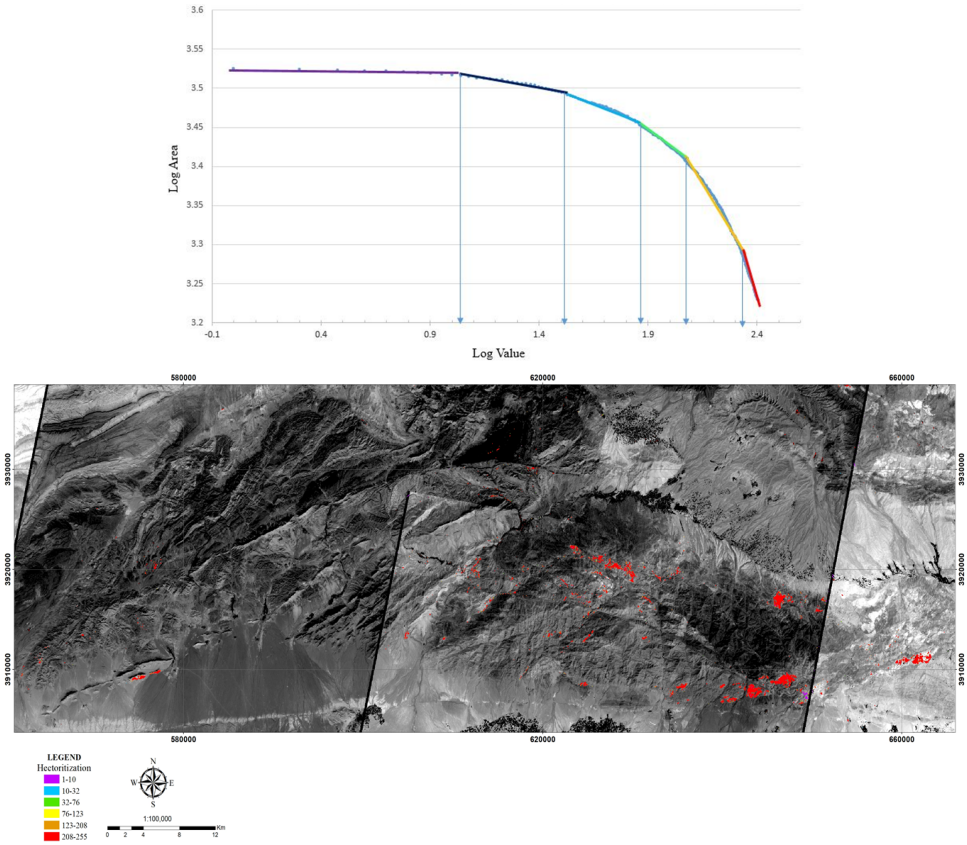

Figure 4. The Log-Log C-A fractal diagram and Second stage of hectorite model based on SAM method.

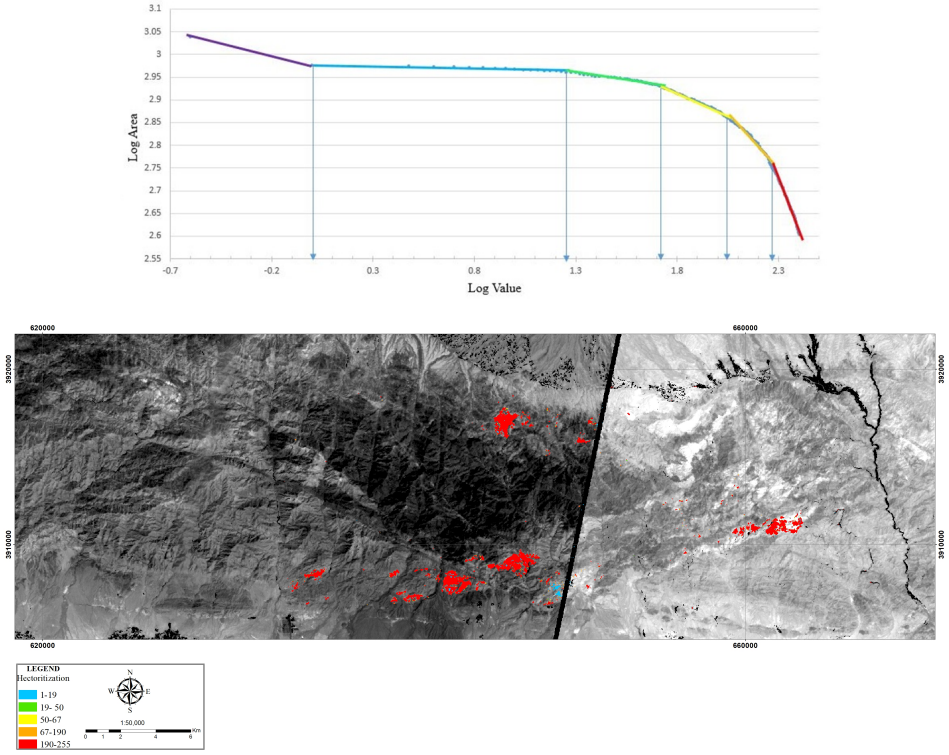

Figure 5. The Log-Log C-A fractal diagram and Third stage of hectorite model based on SFM method.

of the studied area (Figs. 6 and 7), and the results of this analysis are given in Table 1. These results confirm that clay minerals are the most abundant in this part of the range, which is also seen in remote sensing studies and modeling. The most clay minerals in this range, which have been determined by XRD analysis, include illite, montmorillonite and chlorite which are associated with hectorites.

6. conclusion

Stepwise fractal modeling is a new method based on the stepwise factor analysis, which can help in the analysis of various data in order to detect an area with an anomaly

Figure 6. Field observations of clay minerals especially illite, montmorillonite and chlorite in the hectoritic zones.

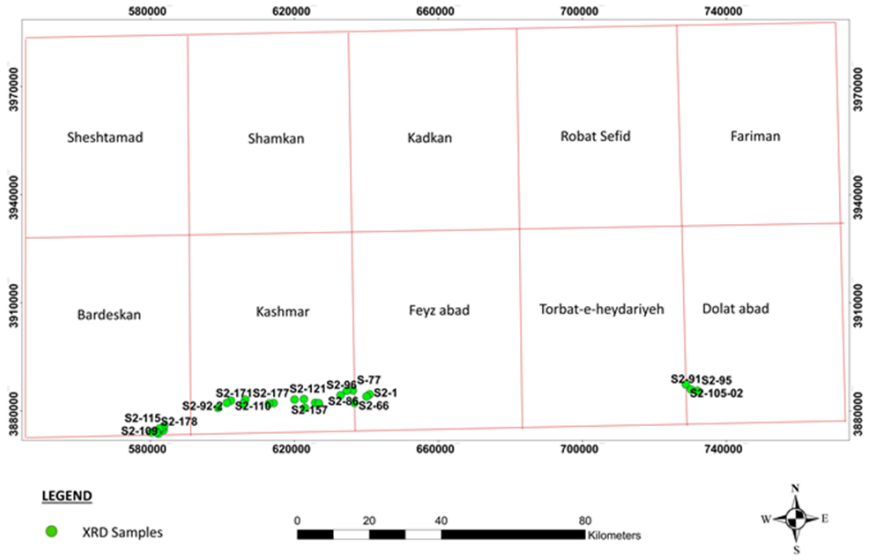

Figure 7. The XRD samples' location map in this region.

and make it smaller and approach the true scale of a large anomaly. This method is useful in categorizing and modeling remote sensing data and could be very effective considering that these data have lithium is one of the strategic elements in high tech and could be fined in various environments such as pegmatites, brains, evaporate rocks such as halite or gypsum and in some clay minerals such as illite, montmorillonite and hectorite. There are significant outcrops of hectorite in eastern parts of Iran in common border with Afghanistan that could be contain the lithium in their Composition and definitely one of the most important exploration targets in Iran.

Table 1. Results of XRD analysis of samples taken from detected areas in remote sensing studies.

Sample	Major Phase (S)	Minor Phase (S)	Trace Phase (S)
S2-198	Quartz/Montmorillonite/Illite	Chlorite/Halite/Orthoclase/Albite	Glauberite/Calcite/Gypsum
S2-110	Gypsum/Quartz/Montmorillonite	Albite/Calcite/Muscovite-illite/Chlorite	Dolomite
S2-42-2	Calcite/Celestine/Montmorillonite/Quartz	Calcite/Montmorillonite/Quartz	——
S2-92-2	Dolomite	Calcite/Montmorillonite/Quartz/Orthoclase	Albite/Gypsum/Celestine/Kaolinite
S2-171	Quartz/Albite/Montmorillonite	Halite/Calcite/Orthoclase/Chlorite	Hematite/Muscovite-illite
S2-1	Calcite/Quartz	Albite/Orthoclase/Muscovite-illite/Chlorite	——
S2-21	Gypsum/Quartz	Montmorillonite/Muscovite-illite/Calcite	——
S-77	Calcite	Quart/Albite/Muscovite-illite/Gypsum	Chlorite/Orthoclase
S2-86	Calcite/Ankerite/Quartz	Albite/Orthoclase/Gypsum/Montmorillonite	Muscovite-illite
S2-66	Calcite/Quartz/Albite	Montmorillonite/Muscovite-illite/ Orthoclase	Chlorite
S2-111	Quartz/Albite/Halite/Calcite	Muscovite-illite/Dolomite/Montmorillonite/Gypsum	Chlorite/Orthoclase
S2-117	Gypsum/Quartz	Calcite/Muscovite-illite/Anhydrite/Albite	Chlorite/Orthoclase/Halite
S2-120	Gypsum/Quartz/Calcite/Anhydrite	Halite/Muscovite-illite/ Montmorillonite/Albite	Chlorite/Orthoclase/Dolomite
S2-124	Gypsum/Quartz	Albite/Calcite/Muscovite-illite/Chlorite	Orthoclase/Halite/Dolomite
S2-157	Anorthite/Calcite	Chlorite/Muscovite-illite/Microcline	Hematite
S2-177	Quartz/Albite/Gypsum/Calcite	Muscovite-illite/Chlorite/Orthoclase	——
S2-96	Gypsum	Chlorite/Muscovite-illite/Albite/Quartz	Calcite/Dolomite

Continued of Table 1.

Sample	Major Phase (S)	Minor Phase (S)	Trace Phase (S)
S2-121	Anhydrite/Gypsum/Dolomite/Celestine	Halite/Quartz/Muscovite-illite/Chlorite	Calcite/Bassanite/Albite
S2-135	Quartz/Albite/ Muscovite-illite	Kaolinite/Calcite/Dolomite/Orthoclase	Hematite
S2-181	Quartz/Albite/ Muscovite-illite/Gypsum	Orthoclase/ Chlorite/Calcite/Hematite	——
S2-102	Gypsum/Quartz/Muscovite-illite	Calcite/Dolomite/Albite/Halite	Chlorite
S2-109	/Quartz/Gypsum/Calcite/Muscovite-illite	Chlorite/Dolomite/Albite/Orthoclase	Halite
S2-115	Quartz/Calcite/Muscovite-illite/Gypsum	Albite/Orthoclase	Chlorite/Dolomite
S2-178	Quartz/Albite/Muscovite-illite	Chlorite/Calcite/Orthoclase/Gypsum	Hematite
S2-178-2	Quartz/Muscovite-illite/Albite	Calcite/Gypsum/Chlorite/Hematite	——
S2-91	Dolomite	Celestine/Quartz/Calcite/Gypsum	Illite
S2-95	Calcite	Celestine/Quartz	——

Authors contributions
Authors have contributed equally in preparing and writing the manuscript.

Availability of data and materials
The data that support the findings of this study are available from the corresponding author, upon reasonable request.

Conflict of interests
The authors declare that they have no known competing financial interests or personal relationships that could have appeared to influence the work reported in this paper.

References

A.A. Zürcher Bookstrom L., Hammarstrom J.M., Mars J.C., Ludington S.D., Zientek M.L., Dunlap P., Wallis J.C. (2019) Tectono-magmatic evolution of porphyry belts in the central Tethys region of Turkey, the Caucasus, Iran, western Pakistan, and southern Afghanistan. *Ore Geology Reviews* 111:102849. DOI: https://doi.org/10.1016/j.oregeorev.2019.02.034.

Afzal P., Abdideh M., Daneshvar Saein L. (2023) Separation of productivity index zones using fractal models to identify promising areas of fractured reservoir rocks. *Journal of Petroleum Exploration and Production Technology,* 1–10. DOI: https://doi.org/10.1007/s13202-023-01657-8.

Afzal P, Farhadi S., Boveiri Konari M., Daneshvar, Shamseddin Meigoony M, Daneshvar Saein L. (2022) Geochemical anomaly detection in the Irankuh District usingHybrid Machine learning technique and fractal modeling. *Geopersia* 12 (1): 191–199. DOI: https://doi.org/10.22059/GEOPE.2022.336072.648644.

Afzal P, Heidari S.M, Ghaderi M, A.B. Yasrebi (2017) Determination of mineralization stages using correlation between geochemical fractal modeling and geological data in Arabshah sedimentary rock-hosted epithermal gold deposit, NW Iran. *Ore Geology Reviews* 91:278–295. DOI: https://doi.org/10.1016/j.oregeorev.2017.09.021.

Aliyari F., Afzal P., Lotfi M., Shokri S., Feizi H. (2020) Delineation of geochemical haloes using the developed zonality index model by multivariate and fractal analysis in the Cu–Mo porphyry deposits. *Applied Geochemistry* 121:104694. DOI: https://doi.org/10.1016/j.apgeochem.2020.104694.

Arjmandzadeh R., Karimpour M.H., Mazaheri S.A., Santos J.F., Medina J.M., Homam S.M. (2011) Sr–Nd isotope geochemistry and petrogenesis of the Chah-Shaljami granitoids (Lut Block, Eastern Iran). *Journal of Asian Earth Sciences* 41:283–296. DOI: https://doi.org/10.1016/j.jseaes.2011.02.014.

Azmi H. (2011) Introduction of Li potentials in Khorasan Razavi, NE Iran. *30th Iranian Symposium of Geosciences, Tehran, Iran,* 7.

Babaei K., Sadeghi B. (2010) Discrimination of alteration zones from ASTER SWIR data in the lead and zinc abandoned area of Rokn-Abad in Ardabil province. *International Mining Congress & Expo, Tehran, Iran*

Bazargani Golshan M., Arian M., Afzal P., Daneshvar Saein L., Aleali M. (2025) Application of fractal models for determining the relationship between REEs and faults in North Kochakali coal deposit, Central Iran. *Scientific Reports* 15 (1): 1276. DOI: https://doi.org/10.1038/s41598-025-85795-5.

Behbahani B., Haratai H., Afzal P., Lotfi M. (2023) Determination of alteration zones applying fractal modeling and Spectral Feature Fitting (SFF) method in Saryazd porphyry copper system, central Iran. *Bulletin of the Mineral Research and Exploration,* DOI: https://doi.org/10.19111/bulletinofmre.1264604.

Cheng Q., Agterberg F.P., Ballantyne S.B. (1994) The separation of geochemical anomalies from background by fractal methods. *Journal of Geochemical Exploration* 51:109–130. DOI: https://doi.org/10.1016/0375-6742(94)90013-2.

Cheng Q., Li Q. (2002) Fractal concentration - area method for assigning a color palette for image representation. *Computers and Geosciences* 28:567–575. DOI: https://doi.org/10.1016/S0098-3004(01)00060-7.

Farhadi S., Afzal P., Boveiri Konari M., Daneshvar Saein L., Sadeghi B. (2022) Combination of Machine Learning Algorithms with Concentration-Area Fractal Method for Soil Geochemical Anomaly Detection in Sediment-Hosted Iran kuh Pb-Zn Deposit, Central Iran. *Minerals* 12:689. DOI: https://doi.org/10.3390/min12060689.

Fyzollahhi N., Torshizian H., Afzal P., Jafari M.R. (2018) Determination of lithium prospects using fractal modeling and staged factor analysis in Torud region, NE Iran. *Journal of Geochemical Exploration* 189:2–10. DOI: https://doi.org/10.1016/j.gexplo.2017.09.017.

Heidari S.M., Afzal P., Sadeghi B. (2024) Molybdenum and gold distribution variances within Iranian copper porphyry deposits. *Journal of Geochemical Exploration,* 107471. DOI: https://doi.org/10.1016/j.gexplo.2024.107471.

Jain R., Sharma R.U. (2019) Airborne hyperspectral data for mineral mapping in Southeastern Rajasthan, India. *International Journal of Applied Earth Observation and Geoinformation* 81:137–145. DOI: https://doi.org/10.1016/j.jag.2019.05.007.

Karimpour M.H., Stern C., Farmer L., Saadat S. (2011) Review of age, Rb-Sr geochemistry and petrogenesis of Jurassic to Quaternary igneous rocks in Lut Block, Eastern Iran. *Geopersia* 1 (1): 19–36. DOI: https://doi.org/10.22059/jgeope.2011.22162.

Kesler S.E., Gruber P.W., Medina P.A., Gregory A., Keoleian M.P. (2012) Everson, Timothy J. Wallington, Global lithium resources: Relative importance of pegmatite, brine and other deposits. *Ore Geology Reviews* 48:55–69.
DOI: https://doi.org/10.1016/j.oregeorev.2012.05.006.

Khalajmasoumi M., Lotfi M., Memar Kochebagh A., Khakzad A., Afzal P., Sadeghi B., Ziazarifi A. (2015) Delineation of the radioactive elements based on the radiometric data using concentration-area fractal method in the Saghand area, Central Iran. *Arabian Journal of Geosciences* 8:6047–6062.
DOI: https://doi.org/10.1007/s12517-014-1610-9.

Khalajmasoumi M., Sadeghi B., Carranza E.J.M., Sadeghi M. (2017) Geochemical anomaly recognition of rare earth elements using multifractal modelling correlated with geological features, Central Iran. *Journal of Geochemical Exploration, Special issue of "Critical metals in the Middle East and North Africa – Geochemistry: Exploration and Analysis"* 181:318–332.
DOI: https://doi.org/10.1016/j.gexplo.2016.12.011.

Koohzadi F., Afzal P., Jahani D., Pourkermani M. (2021) Geochemical exploration for Li in regional scale utilizing Staged Factor Analysis (SFA) and Spectrum-Area (S-A) fractal model in north central Iran. *Iranian Journal of Earth Sciences* 13 (4)
DOI: https://doi.org/10.30495/ijes.2021.685397.

Kruse F.A., Lefkoff A.B., Boardman J.W., Heidebrecht K.B., Shapiro A.T., Barloon J.P., Goetz A.F.H. (1993) The spectral image processing system (SIPS) - Interactive visualization and analyses of imaging spectrometer data. *Remote Sensing of Environment* 44:145–163.
DOI: https://doi.org/10.1016/0034-4257(93)90013-N.

London D. (2008) Pegmatites *Can. Mineral. Spec. Publ.* 10:347.
DOI: https://doi.org/10.2138/am.2009.546.

Malekzadeh Shafaroudi A., M.H. Karimpour, Golmohammadi A. (2013) Zircon U–Pb geochronology and petrology of intrusive rocks in the C-North and Baghak districts, Sangan iron mine, NE Iran. *Journal of Asian Earth Sciences* 64:256–271.

Miri Beydokhti R., Karimpour M.H., Mazaheri S.A., Santos J.F., Klötzli U. (2015) U–Pb zircon geochronology, Sr–Nd geochemistry, petrogenesis and tectonic setting of Mahoor granitoid rocks (Lut Block, Eastern Iran). *Journal of Asian Earth Sciences* 111:192–205.
DOI: https://doi.org/10.1016/j.jseaes.2015.07.028.

Munk L.A., Hynek S.A., Bradley D., Boutt D., Labay K., Jochens H. (2016) Lithium brines: A Global Perspective *Reviews in Economic Geology* 18:339–365. DOI: https://doi.org/10.5382/Rev.18.14.

Pourgholam M.M., Afzal P., Yasrebi A.B., Gholinejad M., Wetherelt A. (2021) Detection of geochemical anomalies using a fractal-wavelet model in Ipack area, Central Iran. *Journal of Geochemical Exploration* 220:106675.
DOI: https://doi.org/10.1016/j.gexplo.2020.106675.

Rahimzadegan M., Sadeghi B., Masoumi M., Taghizadeh Ghalehjoghi S. (2015) Application of target detection algorithms to identification of iron oxides using ASTER images: a case study in the North of Semnan province, Iran. *Arabian Journal of Geosciences* 8:7321–7331.
DOI: https://doi.org/10.1007/s12517-014-1757-4.

Rowan L.C., Mars J. (2003) Lithologic Mapping in the Mountain Pass, California Area Using Advanced Spaceborne Thermal Emission and Reflection Radiometer (ASTER) Data. *Remote Sensing of Environment* 84:350–366.
DOI: https://doi.org/10.1016/S0034-4257(02)00127-X.

Saadati H., Afzal P., Torshizian H., Solgi A. (2020) Geochemical exploration for lithium in NE Iran using the geochemical mapping prospectivity index, staged factor analysis, and a fractal model. *Geochem. Explor. Environ. Anal.* 20:461–472.
DOI: https://doi.org/10.1144/geochem2020-020.

Sabins F. (1999) Remote sensing for mineral exploration.. *Ore Geology Reviews* 14:157–183.
DOI: https://doi.org/10.1016/S0169-1368(99)00007-4.

Sadeghi B. (2021) Simulated-multifractal models: a futuristic review of multifractal modeling in geochemical anomaly classification. *Ore Geology Reviews,*
DOI: https://doi.org/10.1016/j.oregeorev.2021.104511.

Sadeghi B., Afzal P., Moarefvand P., KhodaShenas Firouzabadi N. (2012) Application of Concentration-Area fractal method for determination of Fe geochemical anomalies and the background in Zaghia area, Central Iran *34th International Geological Congress (IGC), Brisbane, Australia.*

Saed S., Azizi H., Daneshvar N., Afzal P., Whattam S.A., Mohammad Y.O. (2022) Hydrothermal alteration mapping using ASTER data, Takab-Baneh area, NW Iran: A key for further exploration of polymetal deposits. *Geocarto International,* 1–25.
DOI: https://doi.org/10.1080/10106049.2022.2059110.

Yazdi Z., Jafari Rad A., Aghazadeh M., Afzal P. (2018) Alteration Mapping for Porphyry Copper Exploration Using ASTER and QuickBird Multispectral Images, Sonajeel Prospect, NW Iran *Journal of the Indian Society of Remote Sensing* 46 (10): 1581–1593.
DOI: https://doi.org/10.1007/s12524-018-0811-1.

Yousefi M., Hronsky J.M.A. (2023) Translation of the function of hydrothermal mineralization-related focused fluid flux into a mappable exploration criterion for mineral exploration targeting. *Applied Geochemistry* 149:105561.
DOI: https://doi.org/10.1016/j.apgeochem.2023.105561.

Yousefi M., Kreuzer O.P., Nykänen V., Hronsky J.M.A. (2019) Exploration information systems–A proposal for the future use of GIS in mineral exploration targeting. *Ore Geology Reviews* 111:103005.
DOI: https://doi.org/10.1016/j.earscirev.2024.104941.